Journal of Alloys and Compounds 504S (2010) S129–S131

Contents lists available at ScienceDirect

Journal of Alloys and Compounds

journal homepage: www.elsevier.com/locate/jallcom

Effect of Co concentration on thermal stability and magnetic properties of (Fe,Co)–Nb–Gd–B glassy alloys

Fei Jia[a], Wei Zhang[a,b,*], Xingguo Zhang[a], Guoqiang Xie[b], Hisamichi Kimura[b], Akihiro Makino[b], Akihisa Inoue[c]

[a] School of Materials Science and Engineering, Dalian University of Technology, Dalian, 116024, China
[b] Institute for Materials Research, Tohoku University, Sendai 980-8577, Japan
[c] Tohoku University, Sendai 980-8577, Japan

ARTICLE INFO

Article history:
Received 30 July 2009
Received in revised form 15 January 2010
Accepted 10 February 2010
Available online 18 February 2010

Keywords:
Metallic glass
Glass transition
Fe-based alloy
Glass-forming ability
Magnetic property

ABSTRACT

A two-stage-like glass transition phenomenon attenuated gradually with an increase in Co content in $(Fe_{1-y}Co_y)_{67.5}Nb_4Gd_{3.5}B_{25}$ (y = 0.1–0.5) glassy alloys, and disappeared for the alloy with y = 0.5, resulting in a large supercooled liquid region of 102 K. As the Co content increases, the liquidus temperature decreases gradually, and the reduced glass transition temperature increases, indicating the enhancement of glass-forming ability (GFA). The best GFA was obtained for alloy with y = 0.5, and the full glassy sample with a diameter of 5 mm could be fabricated by copper mold casting. The (Fe,Co)–Nb–Gd–B glassy alloys exhibited good soft magnetic properties, i.e., rather high saturation magnetization of 0.86–0.91 T, low coercive force below 5.0 A/m, and low saturated magnetostriction of $6–13 \times 10^{-6}$. In addition, the glassy alloys also possessed very high compressive fracture strength of 3821–4112 MPa and high Vickers hardness of 1028–1065.

1. Introduction

Since the synthesis of ferromagnetic bulk glassy alloys (BGAs) in multi-component Fe–(Al,Ga)–(P,C,B,Si) alloy system [1], much effort has been devoted to develop new Fe- and Co-based BGAs exhibiting high glass-forming ability (GFA), high stability of supercooled liquid, excellent soft magnetic properties, good corrosion resistance and high strength. As a result, a large number of ferromagnetic BGAs were developed, and they can be generally classified into five systems, i.e., (Fe, Co)–(Al, Ga)–(P, C, B, Si) [1,2], (Fe, Co)–TM (= Zr, Hf, Mo, Hf, Ta, W)–B [3–5], (Fe, Co)–Ln–B (Ln: lanthanide metal) [6,7], (Fe, Co)–TM–(B, Si) [8,9] and Fe–(P, B, Si) [10]. The $Fe_{62}Co_{9.5}Ln_{3.5}B_{25}$ glassy alloys exhibited larger supercooled liquid region ΔT_x (defined by the difference between glass transition temperature T_g and crystallization temperature T_x) above 50 K and good soft magnetic properties with high saturation magnetization [11]. The addition of a small amount (2 at.%) of Nb to $Fe_{62}Co_{9.5}Ln_{3.5}B_{25}$ alloys increased GFA and ΔT_x [12]. The critical diameter (d_c) for formation of a single glassy phase and ΔT_x value was 1.5 mm and 87 K, respectively [12,13]. Although the GFA increased with further increasing Nb content, a distinct two-stage-like glass transition phenomenon was observed, leading to a decrease in ΔT_x [14]. In this study, with the aim of developing a new ferromagnetic BGA with high GFA and large ΔT_x, we have investigated the effect of Co to Fe concentration ratio on the stability of supercooled liquid, GFA and magnetic properties of $(Fe_{1-y}Co_y)_{67.5}Nb_4Gd_{3.5}B_{25}$ (y = 0.1–0.5) glassy alloy series. In addition, the mechanical properties of the BGAs were also examined.

2. Experimental procedure

The alloy ingots were prepared by arc melting the mixtures of pure Fe, Co, Gd, Nb metals and crystal B with purities of over 99.5 mass% in an argon atmosphere. The alloy ingots were re-melted four times to ensure chemical homogeneity. The mass losses were measured for each ingot after melting and were less than 0.1 mass%. The glassy alloy was produced by injection copper mold casting for bulk cylindrical rods with diameters of 1–7 mm and by melt spinning for ribbons with a cross section of 0.02 mm × 1.2 mm. The structure of the samples was examined by X-ray diffraction (XRD) (CuKα). The thermal stability was examined by differential scanning calorimetry (DSC) at a heating rate of 0.67 K/s. The melting and liquidus temperatures were measured with a differential thermal analyzer (DTA) at a heating rate of 0.17 K/s. Saturation magnetization (I_s) was measured under an applied field of 800 kA/m with a vibrating sample magnetometer (VSM). The dimension of the samples for VSM measurement was 1 mm in diameter and about 10 mm in length. The coercive force (H_c) was measured with a B–H loop tracer by using ribbon samples with the length of about 60 mm. Saturated magnetostriction (λ_s) was measured using a strain gauge with a length of 1 mm at an applied magnetic field of 398 kA/m. Ribbon samples were used for λ_s measurement. All the samples for measurements of magnetic property were annealed for 600 s in the temperature of T_g −80 K to release internal stress. The annealing sample was sealed in a quartz tube, evacuated to 1×10^{-3} Pa, and then isothermally annealed for 600 s at the temperatures

* Corresponding author at: Institute for Materials Research, Tohoku University, Sendai 980-8577, Japan. Tel.: +81 22 215 2470; fax: +81 22 215 2381.
E-mail address: wzhang@imr.tohoku.ac.jp (W. Zhang).

0925-8388/$ – see front matter © 2010 Elsevier B.V. All rights reserved.
doi:10.1016/j.jallcom.2010.02.068

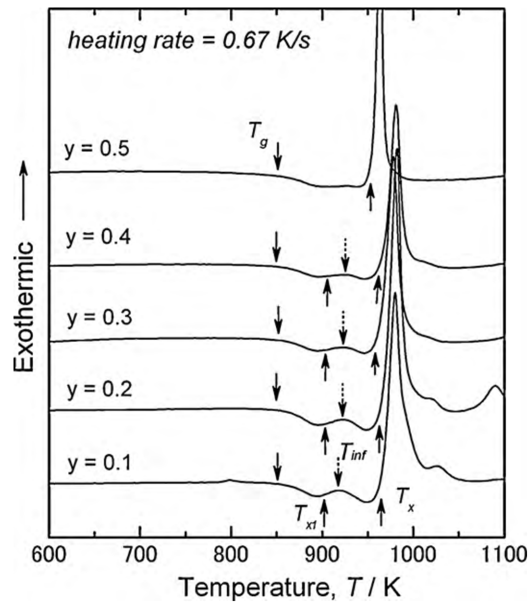

Fig. 1. DSC curves of melt-spun $(Fe_{1-y}Co_y)_{67.5}Nb_4Gd_{3.5}B_{25}$ (y = 0.1–0.5) glassy alloys.

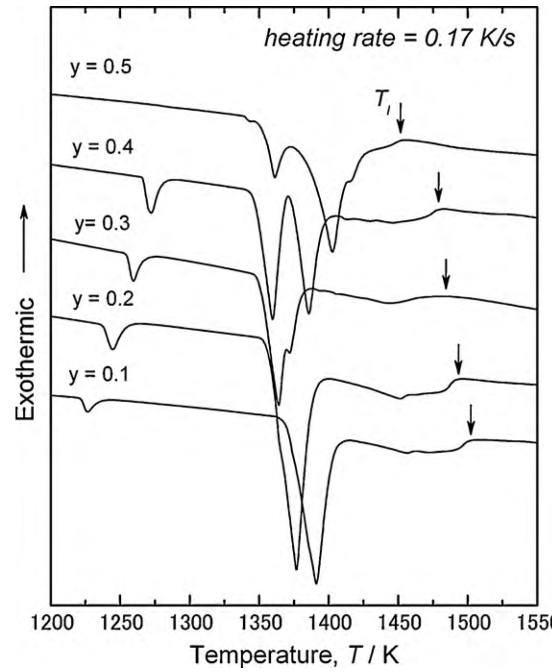

Fig. 2. DTA curves of $(Fe_{1-y}Co_y)_{67.5}Nb_4Gd_{3.5}B_{25}$ (y = 0.1–0.5) alloys.

by an annealing furnace. The mechanical properties under compressive load were measured using an Instron 5581 mechanical testing machine (Instron Corporation, Norwood, MA, USA). The gauge dimension for the mechanical test specimen was 2 mm in diameter and 4 mm in height and its strain rate was fixed as 5.0×10^{-4}/s. The Vicker's hardness (H_v) was measured using a microhardness tester under a load of 25 gf.

3. Results

Fig. 1 shows DSC curves of the $(Fe_{1-y}Co_y)_{67.5}Nb_4Gd_{3.5}B_{25}$ (y = 0.1–0.5) glassy alloys. All the alloys exhibit a distinct glass transition, followed by a supercooled liquid region and then exothermic reactions due to crystallization. However, an additional inflection point (T_{inf}) can be clearly observed in the supercooled liquid region of the alloys with y = 0.1–0.4, which was initially interpreted as a two-stage-like glass transition. This anomalous glass transition phenomenon makes it difficult to decide the ΔT_x value of the glassy alloys. We have investigated the crystalline behavior of $(Fe_{0.9}Co_{0.1})_{67.5}Nb_4Gd_{3.5}B_{25}$ glassy alloy by using XRD, DSC and transmission electron microscopy (TEM). It has been confirmed that a metastable nanoscale $(Fe,Co)_{23}B_6$ phase precipitates in the glassy matrix after annealing, while the two-stage-like glass transition disappears, indicating that the two-stage-like glass transition originates from the exothermic reaction for the precipitation of the $(Fe,Co)_{23}B_6$ phase in the supercooled liquid region [14]. The ΔT_x values of the alloys with y = 0.1–0.4 are determined by the difference between T_g and T_{x1}. It can be also noticed that T_g is almost independent of Co content, while the two-stage glass transition behavior gradually attenuates, and disappears with an increase in Co content to y = 0.5, resulting in a large ΔT_x of 102 K.

Fig. 2 shows DTA curves of the $(Fe_{1-y}Co_y)_{67.5}Nb_4Gd_{3.5}B_{25}$ (y = 0.1–0.5) alloys. Table 1 lists the thermal parameters and d_c of the Fe-based glassy alloys. It can be seen that the liquidus temperature (T_l) decreases gradually from 1498 to 1451 K with increasing Co content from y = 0.1–0.5. This results change in an increase of reduced glass transition temperature ($T_{rg} = T_g/T_l$) form 0.569 to 0.589, indicating enhancement of the GFA [15,16]. Fig. 3 shows the outer shape and XRD patterns of the as-cast $(Fe_{0.5}Co_{0.5})_{67.5}Nb_4Gd_{3.5}B_{25}$ alloy rods. The surfaces of the rods with diameters of 4 and 5 mm are smooth and neither concave nor ruggedness resulting from any crystalline phases is observed (see inset). A shiny appearance typical of a Fe-based BGA can be seen on the fractured surface of the rod with a diameter of 5 mm. The XRD patterns of the samples with diameters of 4 and 5 mm consist only of broad peaks, confirming that a single glassy phase was formed. The further increase in the sample diameter to 6 mm results in the precipitation of crystalline phases. It is therefore concluded that the d_c lies between 5 and 6 mm. The d_c of the other alloys was 3.5 mm at y = 0.2, and 4 mm at y = 0.3 and 0.4.

Table 2 lists the magnetic and mechanical properties of the Fe–Co-based BGAs. It can be seen that all the glassy alloys exhibit

Table 1
The thermal parameters and critical sample diameters of $(Fe_{1-y}Co_y)_{67.5}Nb_4Gd_{3.5}B_{25}$ (y = 0.1–0.5) glassy alloys.

Alloy (at.%)	T_g (K)	T_{x1} (K)	T_x (K)	ΔT_x (K)	T_l (K)	T_{rg}	d_c (mm)
y = 0.1	852	905	962	53	1498	0.569	3.0
y = 0.2	851	907	959	56	1494	0.570	3.5
y = 0.3	855	909	958	54	1486	0.575	4.0
y = 0.4	853	910	963	57	1479	0.577	4.0
y = 0.5	854	–	956	102	1451	0.589	5.0

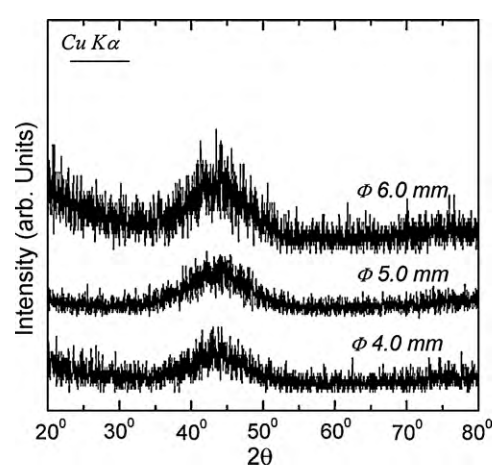

Fig. 3. The cross-sectional XRD patterns of as-cast $(Fe_{0.5}Co_{0.5})_{67.5}Nb_4Gd_{3.5}B_{25}$ alloy rods with diameters of 4, 5 and 6 mm.

Table 2
The magnetic and mechanical properties of $(Fe_{1-y}Co_y)_{67.5}Nb_4Gd_{3.5}B_{25}$ (y = 0.1–0.5) glassy alloys.

Alloy (at.%)	I_s (T)	H_c (A/m)	λ_s (10^{-6})	$\sigma_{c,f}$ (MPa)	E (GPa)	H_v
y = 0.1	0.91	2.5	13	3870	185	1038
y = 0.2	0.92	2.9	11	4112	194	1037
y = 0.3	0.91	3.0	9	3821	184	1028
y = 0.4	0.89	4.5	8	3961	191	1065
y = 0.5	0.86	4.2	6	3854	188	1056

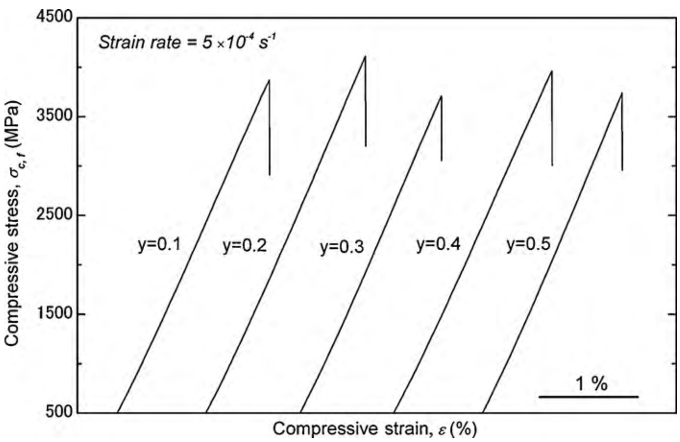

Fig. 4. Compressive stress–strain curves of $(Fe_{1-y}Co_y)_{67.5}Nb_4Gd_{3.5}B_{25}$ (y = 0.1–0.5) glassy alloy rods with a diameters of 2 mm.

good soft magnetic properties, i.e., rather high I_s of 0.86–0.91 T, low coercive force (H_c) below 5.0 A/m, and low saturated magnetostriction (λ_s) of 6–13 × 10^{-6}. Fig. 4 shows compressive stress–strain curves of the Fe-based BGAs. All the alloys exhibit very high fracture strength without a plastic strain. The fracture strength ($\sigma_{c,f}$), Young's modulus (E) and Vickers hardness (H_v) are in the range 3821–4112 MPa, 184–194 GPa, and 1028–1065, respectively, as shown in Table 2.

4. Discussion

The appearance of the two-stage-like glass transition phenomenon may be due to the compositional fluctuation in the (Fe,Co)–Gd–Nb–B glassy alloys. There is a sequent change in atomic sizes among the constituents (Gd 0.180 nm > Nb 0.147 nm > Fe 0.127 nm, Co 0.125 nm > B 0.098 nm) [17], and the strong chemical affinities of Gd–B (−35 kJ/mol), Gd–Fe (−1 kJ/mol), Gd–Co (−22 kJ/mol), Fe–B (−11 kJ/mol), Co–B (−9 kJ/mol), Nb–B (−39 kJ/mol), Nb–Fe (−16 kJ/mol) and Nb–Co (−30 kJ/mol) pairs [18], which contribute to the strengthening of the random networks of trigonal prism-like local unit, leading to enhancement of the stabilization of the supercooled liquid. On the other hand, a large positive heat of mixing between Nb and Gd (30 kJ/mol) [18] is also contributed to repulsive chemical interactions in the system, which may result in the local compositional fluctuation in the supercooled liquid [19], leading to the two-stage-like glass transition. With increasing Co content, the two-stage glass transition behavior gradually attenuates, and almost disappears for an alloy with y = 0.5 (see Fig. 1). It seems to be caused by the lowering of repulsive chemical interactions with the Nb–Gd pair. Because the Gd–Co and Nb–Co pairs have larger negative heat of mixing than those of Gd–Fe and Nb–Fe pairs, respectively. With increasing the concentration ratio of Co to Fe, the chemical affinities will be increased relatively between the Gd and Nb elements, which may decrease repulsive chemical interactions between Nb and Gd. As a result, the compositional fluctuation in the glassy alloys is reduced, and the two-stage glass transition is gradually disappeared.

It has been noticed that the best GFA of the alloy with y = 0.5 shows a lowest T_l of 1451 K and highest T_{rg} of 0.588 in the alloy series. This implies that the viscosity of the supercooled liquid increases rapidly with decreasing temperature. It is well known that this rapid increase is favorable for easy solidification of supercooled liquid into a glassy solid state under the suppression of crystallization reaction.

It has also been noticed that the lower λ_s values are obtained for the alloys with higher Co contents. It can be considered that the λ_s of the glassy alloys has a close relation to Co concentration because the Co-based glassy or amorphous alloys exhibited nearly zero λ_s [20]. The similar decrease in λ_s with increasing Co content has been recognized for other Fe–Co-based glassy alloy systems [20,21].

5. Conclusions

A two-stage-like glass transition phenomenon was obtained for $(Fe_{0.9}Co_{0.1})_{67.5}Nb_4Gd_{3.5}B_{25}$ glassy alloy, attenuated gradually with increasing Co content in $(Fe_{1-y}Co_y)_{67.5}Nb_4Gd_{3.5}B_{25}$ (y = 0.1–0.5) glassy alloys, and disappeared for the alloy with y = 0.5. The large ΔT_x of over 100 K was obtained for the alloys with y = 0.5. The GFA of the alloys increased with increasing Co content. The best GFA was also obtained for the alloy with y = 0.5, and the full glassy samples with diameters up to 5 mm could be fabricated by copper mold casting. The $(Fe_{0.5}Co_{0.5})_{67.5}Nb_4Gd_{3.5}B_{25}$ glassy alloy exhibited rather high saturation magnetization of 0.86 T, low coercive force of 4.2 A/m, low saturated magnetostriction of 6 × 10^{-6}, high fracture strength of 3854 MPa, and high Vickers hardness of 1056. The high GFA, large ΔT_x, excellent soft magnetic properties and high fracture strength give the new BGA engineering applications as functional materials.

Acknowledgements

This work was financially supported by Research and Development Project on Advanced Metallic Glasses, Inorganic Materials and Joining Technology from the Ministry of Education, Science, Sports, and Culture of Japan.

References

[1] A. Inoue, J.S. Gook, Mater. Trans. JIM 36 (1995) 1180.
[2] A. Inoue, A. Katsuya, Mater. Trans. JIM 37 (1996) 1332.
[3] A. Inoue, T. Zhang, T. Itoi, A. Takeuchi, Mater. Trans. JIM 38 (1997) 359.
[4] A. Inoue, T. Zhang, A. Takeuchi, Appl. Phys. Lett. 71 (1997) 464.
[5] P. Pawlik, H.A. Davies, M.R.J. Gibbs, Appl. Phys. Lett. 83 (2003) 2775.
[6] W. Zhang, A. Inoue, Mater. Trans. JIM 41 (2000) 1679.
[7] C.Y. Lin, H.Y. Tien, T.S. Chin, Appl. Phys. Lett. 86 (2005) 16250.
[8] A. Inoue, B.L. Shen, Mater. Trans. 43 (2002) 766.
[9] C.T. Chang, B.L. Shen, A. Inoue, Appl. Phys. Lett. 88 (2006) 011901.
[10] A. Makino, T. Kubota, C. Chang, M. Makabe, A. Inoue, J. Magn. Magn. Mater. 320 (2008) 2499.
[11] W. Zhang, A. Inoue, Mater. Trans. 42 (2001) 1142.
[12] Y. Long, W. Zhang, X. Wang, A. Inoue, J. Appl. Phys. 91 (2002) 5227.
[13] W. Zhang, Y. Long, M. Imafuku, A. Inoue, Mater. Trans. 43 (2002) 1974.
[14] W. Zhang, F. Jia, X. Zhang, G. Xie, H. Kimura, A. Inoue, J. Phys. Appl. 105 (2009) 053518–53521.
[15] D. Turnbull, Contempt. Phys. 10 (1969) 473.
[16] A. Inoue, Acta. Mater. 48 (2000) 279.
[17] Japan Inst. Metals (Ed.), Metals Databook, Maruzen, Tokyo, 1983 (pp. 8).
[18] F.R. Niessen, Cohesion in Metals, Elsevier Science Publishers, Amsterdam, 1988, p. 219.
[19] Y. Hirotsu, T. Hanada, T. Ohkubo, A. Makino, Y. Yoshizawa, T.G. Nieh, Intermetallics 12 (2004) 1081.
[20] K. Amiya, A. Urata, N. Nishiyama, A. Inoue, J. Appl. Phys. 101 (2007), 09N112-1.
[21] H. Koshiba, A. Inoue, Mater. Trans. 42 (2001) 2572.